THE JOURNAL OF PHYSICAL CHEMISTRY A

ARTICLE

pubs.acs.org/JPCA

Molecular Modeling of Organophosphorous Agents and Their Aqueous Solutions

Aleksey Vishnyakov, Gennady Yu. Gor, Ming-Tsung Lee, and Alexander V. Neimark*

Department of Chemical and Biochemical Engineering, Rutgers, the State University of New Jersey, 98 Brett Road, Piscataway, New Jersey 08854, United States

Supporting Information

ABSTRACT: Using molecular dynamics simulations, we modeled solvation and diffusion in aqueous solutions of organophosphorous compounds, including nerve G-agents sarin and soman (methylphosphonofluoridates) and their common simulants DMMP (dimethyl methylphosphonate) and DIFP (diisopropyl fluorophosphate). The aqueous solutions of the organophosphorous compounds were found to display complex molecular scale structures and dynamic properties due to competing interactions between strongly hydrophobic and hydrophilic groups. The mixing of agents with water was proved to be exothermic with negative excess mixing volume, indicating a strongly hydrophilic solvation. This effect was confirmed in a specially performed experiment. We discuss to what extent DMMP and DIFP are suitable simulants for G-agents in experimental studies, as far as their interactions with water are concerned. We also focus on the relevance of the structural features and mobilities of agents in water to their interactions with permselective polyelectrolyte membranes that may be employed as protective barriers against chemical warfare agents.

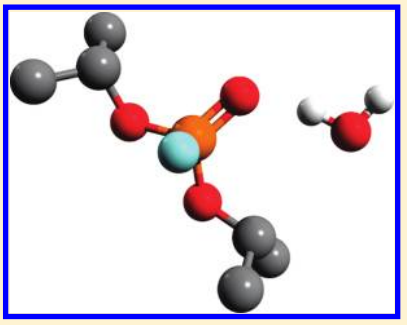

I. INTRODUCTION

The increasing concern regarding the risk of terrorist attacks involving chemical warfare agents (CWAs),[1−3] such as G-agents sarin and soman (Figure 1a,c), has intensified the studies of organophosphorous compounds. In particular, understanding of the specifics of thermodynamic and transport behavior of these compounds in aqueous environments is crucial. Molecular dynamics (MD) modeling of agent−water mixtures is the subject of the current paper.

Because of the extreme toxicity of CWAs, most experimental studies of reactivity, sorption, and transport are performed with their less toxic simulants. Thus, it is important to understand to what extent a simulant mimics the agent properties and to evaluate which simulant would be best suited for a particular situation. DMMP (dimethyl methylphosphonate, Figure 1b) and DIFP (diisopropyl fluorophosphate, Figure 1d) are two simple compounds that are used as simulants to mimic the reactivity and transport of sarin and soman. The molecular size and chemical structure of the simulants resemble the size and chemistry of the corresponding nerve agents. Though similar to real G-agents, they do not include the "core" methylflourophosphonate group, which is simulated by methylphosphonate and fluorophosphate groups in DMMP and DIFP, respectively. That is, either fluorine or methyl bonded to the phosphorus atom of the G-agent is replaced by an alkoxy group in the simulant. DMMP is a compound of low toxicity with a wide range of industrial applications, while DIFP is a potent neurotoxin, although much weaker than G-agents. It is worth noting that sarin and soman contain chiral phosphorus atoms, and soman also has a chiral carbon, while both DMMP and DIFP are symmetric molecules with no stereoisomers possible.

Unlike alkylphosphates that are found in biological macromolecules, alkylphosphonates and fluorophosphates and their aqueous solutions received relatively little attention from both experimentalists and theoreticians. Thermodynamic and dielectric properties of lower alkylphosphonates including DMMP were studied back in 1950s.[4−7] The dielectric constants obtained allowed the authors to speculate on preferential conformations of lower alkylphosphonates: in particular, "extended" and "folded" geometries were described.[4,6] In 1985 the first ab initio study of *O*-methyl methylphosphonofluoridate, a smaller homologue of sarin, was published by Ewig and van Wazer.[8] Suenram et al[9,10] thoroughly studied the conformations of DMMP and sarin molecules in vacuum using Fourier-transform microwave spectroscopy and ab initio Hartree−Fock (HF) and Møller−Plesset (MP) calculations. Ault et al.[11] studied DMMP interactions with water from infrared (IR) spectra obtained both experimentally and using ab initio minimizations. The authors estimated the energy of hydrogen bond formation between water and DMMP molecules and examined the influence of the hydrogen bond formed to the stretching frequencies of P═O and O —H bonds. Recently Bermudez published a series of ab initio studies of absorption of DMMP and sarin on various surfaces.[12−14] In ref 13, different levels of theory were tested on reproducing IR spectra of pure DMMP and sarin, showing that the DFT/B3LYP

Received: January 17, 2011
Revised: April 17, 2011
Published: May 04, 2011

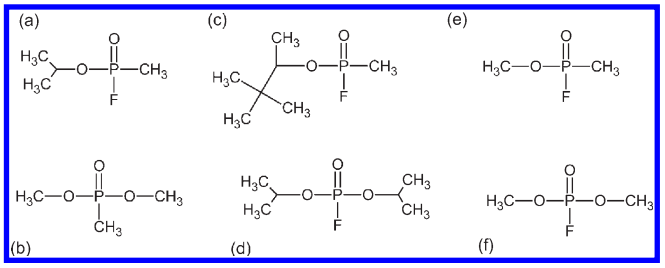

Figure 1. Molecules considered in this paper. (a) sarin (GB, *O*-isopropyl methylphosphonofluoridate, an organophosphorous CWA) (b) dimethyl methylphosphonate (DMMP, simulant for G-agents) (c) soman, (GD, *O*-pinacolyl methylphosphonofluoridate, an organophosphorous CWA), (d) diisopropylfluorophosphate (DIFP, a simulant for G-agents) (e) *O*-methyl methylphosphonofluoridate (f) dimethylfluorophosphate (hereinafter DMFP). The last two compounds were used for fitting the components of the forcefield.

level of theory is suitable for such calculations. The same level of theory is used in our calculations. Early simulations of bulk alkylphosphonates published in the literature[15−19] employed generic forcefields. Vishnyakov and Neimark[20] developed a molecular model specific to DMMP that reproduced reasonably the conformations and experimental properties of DMMP and its aqueous solutions. This model was later employed in studies of DMMP diffusion in Nafion.[21] Sokkalingam, Kamath, Coscione, and Potoff[22] extended the original transferable potential for phase equilibria (TraPPE) forcefield to alkylphosphonates and modeled the bulk vapor−liquid equilibrium (VLE) for pure sarin, soman, and DMMP. The authors[22] achieved a very good agreement between the experimental and Monte Carlo phase diagrams of the pure liquids, but they did not model the aqueous solutions of the CWA and simulants. The forcefield from ref 22 is further on referred to as SKCP and the DMMP model from ref 20 is referred to as VN.

The work presented here was motivated by the intent to study the mechanisms of G-agent and simulant transport through hydrated permselective polyelectrolyte membranes, which are being explored as protective barrier materials.[23] Our work had three main purposes: (1) explore the interactions of G-agents and their simulants with water; (2) reveal the relation between the specifics of solvation of G-agents and simulants and their self-diffusion in aqueous solutions; (3) from comparison between the G-agents and simulants, understand how well simulants (DMMP, DIFP) mimic actual agents in different aspects that may be relevant to their transport in hydrated polyelectrolyte membranes.

In section II, we extend the SKCP forcefield for G-agents and DMMP to fluorophosphates, of which DIFP and dimethylfluorophosphate (DMFP) are typical examples. To remedy a lack of experimental data on aqueous solutions of agents required for validation of the forcefields, we performed the measurements of densities and excess mixing volumes of aqueous solutions of DMMP presented in section III. Section IV is devoted to the description of molecular dynamics simulations. In section V, we discuss thermodynamic properties of G-agents and simulants in aqueous solutions and compare the simulation results with the experimental data. In section VI, we discuss the self-diffusion of agents and water and relate the transport properties to the molecular structure of agent solutions. A summary of the results is given in section VII.

II. DERIVATION OF THE MOLECULAR FORCEFIELD FOR FLUOROPHOSPHATES

We employed the SKCP forcefield[22] in simulations of G-agents and DMMP. We also performed a few simulations of DMMP solutions with the VN model,[20] which gave results comparable with the SKCP model. Because fluorophosphates (such as DIFP and DMFP) were not considered in these works,[20,22] we developed a united-atom forcefield for this group of compounds by fitting the forcefield terms for fluorophosphate groups, which are not present in sarin and DMMP, to the conformations that were DFT-optimized with cc-pvdz basis set[24] and B3LYP[25,26] exchange correlation functional. The forcefield terms are presented in Table 1; atomic partial charges are given in Table 2. We also determined the stiffness of covalent bonds to make the models applicable to unconstrained simulations (in refs 20 and 22 all bond lengths were kept constant). PQS ab initio package[27] was employed for minimization. To simplify the parameter fitting for bonds, angles, and dihedrals, we performed optimization on *O*-isopropyl methylphosphonofluoridate and DMFP, instead of sarin and DIFP (Figure 1), where possible. First, we found the optimal conformations of the compounds. Then bond stiffness was determined by scanning the energy dependence on the bonds lengths. The covalent angles were fitted by perturbing the angles around the phosphorus atom by less than 7°, with the basic conformations kept intact, in order to avoid a significant contribution from the torsion angles. Then the equilibrium angle θ_0 and bending stiffness K_θ parameters were fitted to the ab initio energies.

The only dihedral term specific to DMFP and DIFP describes the rotation of the alkyl end groups around single P−O bonds. Following the SKCP approach[22] that used a single dihedral angle to describe the rotation of each alkyl end group, we chose the F−P−O−C dihedral angle for this purpose (O═P—O—C and O—P—O—C torsion energies were set to zero). The F—P—O—C parameters were determined by a standard procedure: we rotated the methyl group of the DMFP molecule around the P−O single bond and minimized the structure with the torsion angle fixed at different positions. For all other terms were by that point already determined, the F—P—O—C torsion parameters were fit to this ab initio energy profile (Figure 2).

Our forcefield for fluorophosphates accurately reproduces the conformations of DMFP and reasonably reproduces the conformations of DIFP. The level of agreement between the empirical forcefield and ab initio calculations is similar to that in ref 22. Both compounds have several conformations with very close energies. The comparison between ab initio and classical energies for the main conformations is shown in Figure 3. The deviation of the classical energy of the fourth DIFP conformation from ab initio value is mainly due to high Coulomb interactions, relative to the three other.

As an additional test of our forcefield, we performed the molecular mechanics calculations for interactions of DIFP with one water molecule. Calculations were provided using the Gromacs molecular dynamics package.[28] DIFP oxygen tends to form a hydrogen bond with the water hydrogen (configuration from our calculations is given in Figure 4a). The O···H distance is 1.69 Å and the bonding energy is 9.7 kcal/mol. These parameters for water−water interactions are 1.72 Å and 7.6 kcal/mol, respectively; and for DMMP−water (using the SKCP forcefield from ref 22) are 1.60 Å and

Table 1. Parameters of the Potential Models of DIFP[a]

potential	model	parameters		
stretching	$E_b(l) = K_b(l - l_0)^2$		l_0 (Å)	K_b (kJ mol^{-1} Å^{-2})
		O═P	1.48	3051.33
		F−P	1.630	1350.99
		O−P	1.614	1445.80
		C−O[46]	1.473	1720
		C−C[46]	1.520	944
bending	$E_\theta(l) = K_\theta(\theta - \theta_0)^2$		θ_0 (deg)	K_θ (kJ mol^{-1} rad^{-2})
		O═P−F	113.00	273.61
		O═P−O	117.44	287.73
		F−P−O	101.72	300.76
		O−P−O[22]	103.22	259.69
		C−O−P[22]	120.66	334.83
		C−C−O[22]	107.40	259.69
		C−C−C[22]	113.99	259.69
torsional	$E = \Sigma_{i=0}^{5} a_i \cos^i\varphi$	F−P−O−C	a_i (kJ mol^{-1})	
			$a_0 = 50.131$	
			$a_1 = -7.103$	
			$a_2 = 2.628$	
			$a_3 = 13.729$	
			$a_4 = -4.339$	
			$a_5 = -5.520$	
torsional	$E = c_0$			
	$+ c_1[1 + \cos(\varphi + f)]$	C−C−O−P[22]	c_i (kJ mol^{-1})	
	$+ c_2[1 + \cos(2(\varphi + f))]$		$c_0 = 8.653$	
	$+ c_3[1 + \cos(3(\varphi + f))]$		$c_1 = -6.257$	
			$c_2 = 3.590$	
			$c_3 = 1.886$	
			$f = 1.88$	

[a] The 1−4 nonbonded atom interactions (that is Lennard-Jones and Coulomb between the atoms separated by three covalent bonds) scaled by the factor of 0.5, generally applied in TraPPE forcefield. Lennard-Jones parameters for interaction between unlike bodies calculated using the standard Lorentz−Berthelot mixing rules.[22] Atomic partial charges for the molecules considered in this paper are presented in Table 2. Additional details on fitting of the forcefield terms presented in Table 1 are given in Supporting Information.

11.5 kcal/mol. Configuration of the hydrogen-bonded DIFP−water cluster is given in Figure 4b. While both our forcefield and SKCP forcefield predict energy values which deviate from the complexation energies obtained using ab initio calculations at the level of theory used above (DIFP−water 4.6 kcal/mol, and DMMP−water 5.9 kcal/mol), they demonstrate the correct trend for hydrogen bond formation, while comparing DIFP against DMMP, and predict the cluster geometries consistent with the ones obtained from ab initio calculations.

Adding the second water molecule to the DIFP−water pair leads most likely to the formation of water−water hydrogen bonding, while the second water molecule is not be bonded to DIFP (Figure 4c). The same cluster was predicted with using ab initio calculations. As in the case of one water molecule, molecular mechanic calculations give shorter bond length bonding: bond length between DIFP and water is 1.62 Å (ab initio value is 1.85 Å) and between two water molecules is 1.68 Å (ab initio value is 1.93 Å).

III. EXPERIMENTAL MEASUREMENT OF THE EXCESS MIXING VOLUME IN DMMP−WATER SOLUTIONS

Validation of the molecular models of organophosphorous compounds under consideration is hindered by a scarcity of experimental data on thermodynamic properties of their aqueous solutions. In order to enable a quantitative comparison with reliable experimental data, we measured the concentration dependence of the density of the DMMP aqueous solution and calculated the excess mixing volume. DMMP liquid of 99.5% purity was obtained from Pfaltz&Bauer and used without further purification. The densities of DMMP liquid at 25 °C reported in materials safety data sheets of different producers range from ρ = 1.145 to 1.161 g/cm^3. The measured density ρ = 1.1592 g/cm^3 was close to the upper limit of this range. Starting from pure water, we made a number of reference solution samples of approximately 20 cm^3 each, measuring the amount by volume, and determined the densities (shown in Figure 5) with the oscillatory specific gravity meter DMA 35N from Anton Paar. The excess mixing volume at the DMMP molar fraction x_P was calculated as

$$\Delta\tilde{V}_{mix} = [M_P x_P + M_W(1 - x_P)]/\rho(x_P) - M_P x_P/\rho_P - M_W(1 - x_P)/\rho_W \quad (1)$$

where M_P and ρ_P are the molar mass and density of pure agent, and subscript "W" denotes the same properties of water. The dependence of $\Delta\tilde{V}_{mix}$ on the composition is given in Figure 6a. The experimental error is 0.0010 g/cm^3.

dx.doi.org/10.1021/jp200509u |J. Phys. Chem. A 2011, 115, 5201–5209

Table 2. Partial Charges and Lennard-Jones Interaction Parameters for the Molecules Considered in This Paper[a]

	partial atomic charges, q (e)						LJ parameters	
atom	sarin	DMMP	soman	DIFP	short sarin[b]	DMFP	ε (K)	σ (Å)
P	1.35	1.16	1.26	1.56	1.46	1.20	86.0	4.00
O (=P)	−0.68	−0.66	−0.67	−0.72	−0.76	−0.6	79.0	3.05
F	−0.36		−0.33	−0.36	−0.34	−0.26	26.7	2.95
O	−0.59	−0. 41	−0.52	−0.67	−0.45	−0.4	55.0	2.80
CH_3	−0.11	0.21	−0.1	−0.1	0.23	−0.23	98.0	3.75
CH	0.61		0.31	0.63			10.0	4.33
CH_3 (−P)	−0.11	−0.1	−0.06		−0.14		98.0	3.75
C			0.71				0.5	6.40
CH_3 (−C)			−0.20				98.0	3.75

[a] Charges were obtained using CHELPG orbital population analysis of the results of restricted Hartree−Fock optimization with cc-pvdz basis set. Lennard-Jones parameters were adopted from ref 22. [b] *O*-Methyl methylphosphonofluoridate.

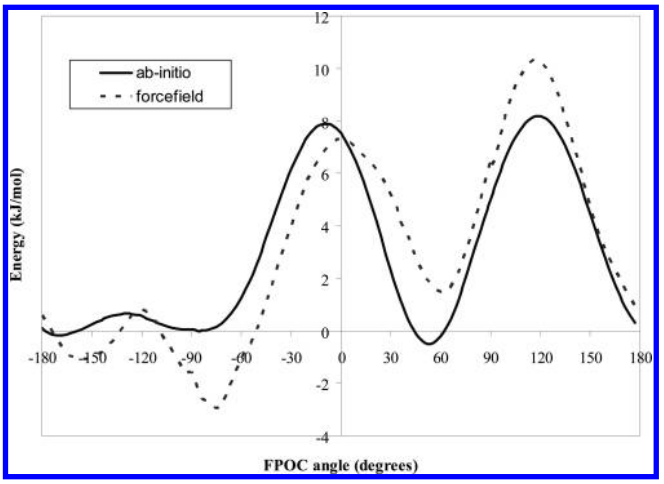

Figure 2. The energy of DMFP molecule as a function of FPOC torsion angle: solid curve, ab initio calculations; dashed curve, forcefield.

The experimental density exceeds the density of the corresponding ideal mixture throughout the entire concentration range, indicating a strongly hydrophilic solvation. The DMMP mixing volume has a smooth minimum at 40% mol DMMP (80 wt %). The excess mixing volume reaches −0.775 mL/mol, which is close to that of dimethyl sulfoxide (DMSO) (refs 29 and 30, data taken from ref 31), which is a hydrophilic organic liquid that has a double-bonded oxygen in the hydrophilic group and two methyl groups, similar to DMMP. The thermodynamic properties of DMSO solutions show an exception at 25 mol % DMSO: for example, the freezing temperature has a sharp minimum at this concentration. This leads to suggestions that stable 1:3 DMSO/water complexes[32] are formed in DMSO aqueous solutions. In contrast, the smooth minimum of $\Delta\tilde{V}_{mix}$ at 40 mol % for DMMP does not suggest any semistable complexes in our system. The collected experimental data on DMMP solutions is used for comparison with the calculation results in section V.

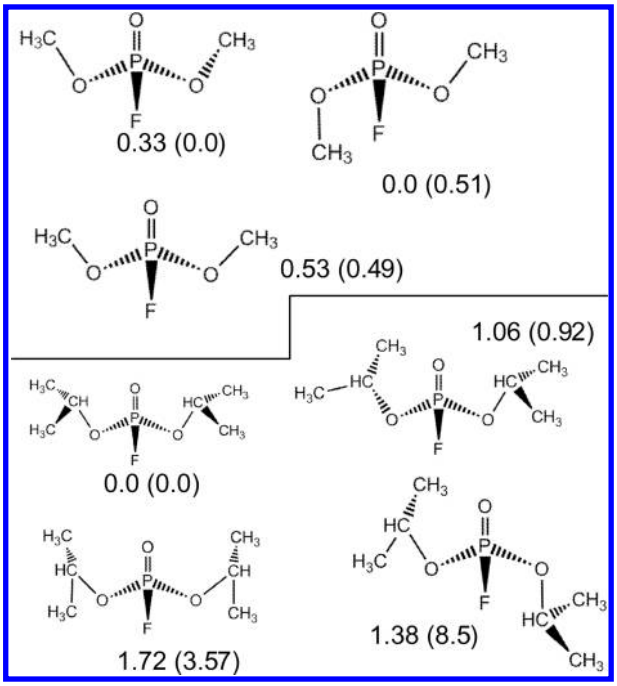

Figure 3. Comparison between the energies (in kJ/mol) of energy-optimized conformers of DMFP and DIFP predicted by B3LYP DFT with cc-pvdz basis and by empirical forcefield (in brackets). The optimal conformation of each molecule assumed as zero.

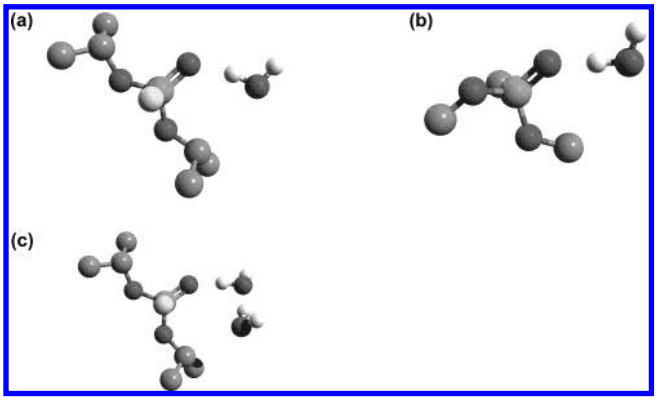

Figure 4. Small simulant−water clusters obtained by molecular mechanics calculations: (a) DIFP−water; (b) DMMP−water (SKCP forcefield[22]); (c) DIFP with two water molecules, forming one hydrogen bond with the DIFP. Hydrogen atoms are not represented in the simulants molecules, since united-atom models are used.

IV. MOLECULAR DYNAMIC SIMULATIONS

The MD simulations were carried out using the MDynaMix 5.0 program[33] at constant temperature of T = 296.2 K and pressure of p = 1 atm (that is, in NPT ensemble). Water was modeled by a rigid three-center SCP/E model of Berendsen et al.[34] Initially, the molecules were placed in a 3D periodic cubic simulation cell at a low density of ρ = 0.05 g/cm^3 and gradually compressed in a series of NVT and/or NPT MD runs to a liquid-like density of ρ = 1.0 g/cm^3. The number of molecules in each system was chosen so that the box size of approximately 40 Å would be obtained. One may assume that the limited system size may influence the diffusion coefficients, which may be somewhat

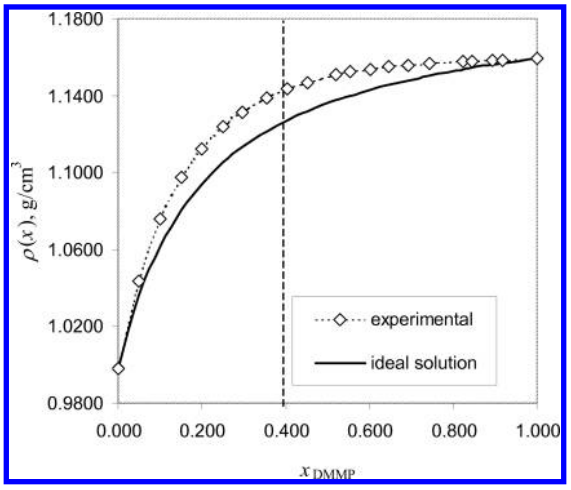

Figure 5. Experimental densities of DMMP−water solutions compared with those from ideal approximation. The vertical dashed line indicates the location of the minimum value of the excess mixing volume.

larger in an infinite system. We tried to keep the system size constant in order to make correct comparisons. Conformations and orientations in the initial configuration were chosen randomly. The compression stage was followed by 300−800 ps NPT equilibration runs, after which statistics were collected over 400−1600 ps averaging run for each system. The equations of motion were solved using the Verlet[35] leapfrog algorithm using the double time step integration scheme of Tuckerman.[36] A time step of 0.1 fs was applied to fast-fluctuating bond stretching and angle bending forcefield terms. "Long" timesteps applied to all other interactions were varied with the system from 0.3 to 2.0 fs, in order to ensure a proper convergence of the integration algorithm. Temperature and pressure were maintained using the Nose-Hoover[37,38] thermostat. The thermostat relaxation time was set to 30 ps, and the barostat relaxation time was set to 800 fs.

Table 3 shows the physical properties of pure liquids. The densities and heats of evaporation for sarin, soman, and DMMP are in a reasonable agreement with those reported in ref 22 except for the density of sarin, which turned out to be lower in our simulations, although there is no general tendency to the lower densities. The densities of all compounds but DMMP are somewhat overestimated compared to the experiment. The diffusion coefficients of pure liquids generally follow the obvious trend: diffusion becomes slower as the molecular size increases. We have to note that a faster diffusion was obtained with the SKCP model compared to the VN model, perhaps because of a more accurate description of molecular conformations that were fitted to a wider array of ab initio energies and geometries. It should be noted that DMFP, despite apparent similarities to DMMP as far as the molecular size and functional groups are concerned, exhibits a much lower heat of evaporation and a much faster self-diffusion. The boiling point of DMFP is relatively low (99 °C compared to 180 °C for DMMP), and its saturated vapor pressure is relatively high, 5.9 kPa.[40] Similarly to the effect observed in the DMFP−DIFP homologue pair, *O*-methyl methylphosphonofluoridate, a smaller homologue of sarin (Figure 1e), has a much higher liquid density. However, its self-diffusion coefficient is only moderately faster and the heat of evaporation exceeds that of sarin (Table 3). Unfortunately, we did not find any experimental reference

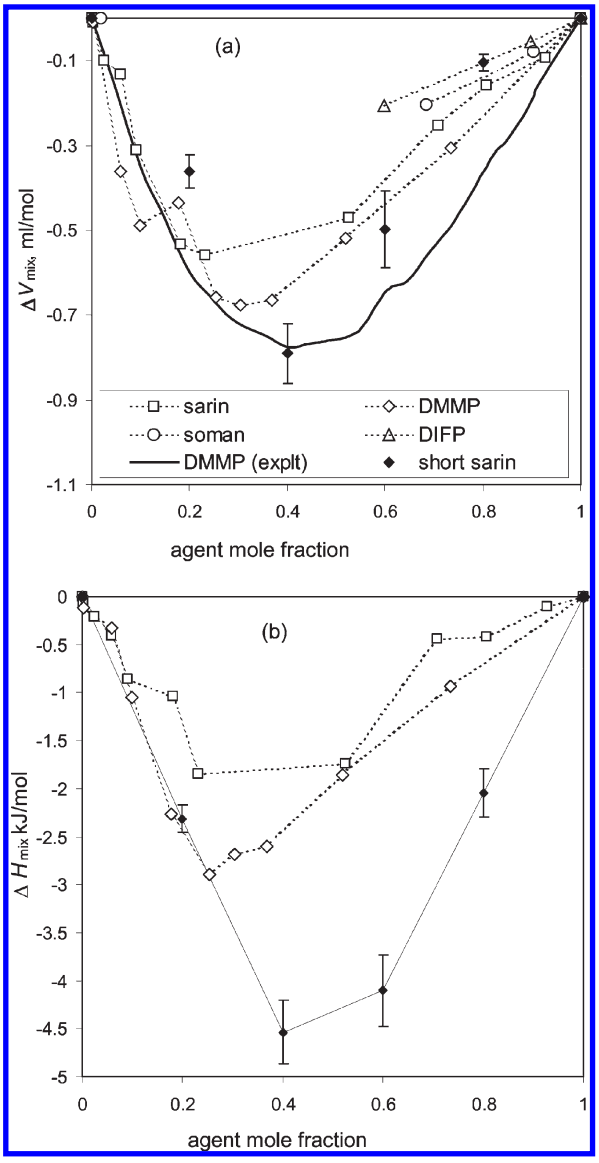

Figure 6. Excess mixing volume (a) and enthalpy (b) for the mixtures of soman, sarin, *O*-methyl methylphosphonofluoridate, DMMP, and DIFP with water. Water−soman and water−DIFP mixtures show phase separation at water fraction higher than 0.4; therefore the data for this system are not shown in the figure.

for *O*-methyl methylphosphonofluoridate to compare our calculations with.

Overall, we simulated 42 different systems, from pure chemicals to dilute solutions in water. It should be mentioned that DMMP is miscible with water at ambient conditions, and the same likely applies to sarin. However, soman and DIFP are poorly soluble (at 2.1×10^4 and 1.53×10^4 mg/l at 25 °C, respectively[39]), although water has a high solubility in soman, about 18%,[40] and DIFP is likely to behave similarly. Sarin−water, DMMP−water, and *O*-methyl methylphosphonofluoridate−water solutions were considered in the entire range of compositions. DIFP−water and soman−water solutions were only modeled at the compositions corresponding to the uniform liquid according to the experimental data.

dx.doi.org/10.1021/jp200509u |*J. Phys. Chem. A* 2011, 115, 5201–5209

Table 3. Physical Properties of Pure Sarin, Soman, DMMP and DIFP Obtained by Molecular Dynamics Simulations: Density, Diffusion Coefficient, and Enthalpy of Evaporation at 296.2 K

compound	ρ, g/cm^3, MD	ρ, g/cm^3, expt	$10^9 D$, m^2/s	ΔH_{evap}, kJ/mol (MD)	ΔH_{evap}, kJ/mol (expt) at 298 K
sarin	1.129	1.088[47]	0.45	48.3	46.9[47]
short sarin[a]	1.258		0.58	49.3	
DMMP (SKCP)	1.156	1.151[6]	0.45	53.8	52.25[6,8]
DMMP (VN)	1.156[20]	1.151[6]	0.39 (0.5[b])	50.2	52.25[6,8]
soman	1.046	1.022[47]	0.34	54.7	55.2
DMFP	1.236	1.232[48]	1.37	37.1	
DIFP	1.0714	1.055[49]	0.31	53.8	

[a] *O*-Methyl methylphosphonofluoridate. [b] NMR data from refs 44 and 45 at 293 K.

V. THERMODYNAMIC PROPERTIES

From the densities and energies obtained in the MD simulations, we obtained the excess mixing volumes $\Delta\tilde{V}_{mix}$ and enthalpies $\Delta\tilde{H}_{mix}$. The mixing enthalpies were calculated as

$$\Delta\tilde{H}_{mix} = E - E_P x_P - E_P(1 - x_P) + p\Delta\tilde{V}_{mix} \qquad (2)$$

They are shown in Figure 6, together with the experimental results for the water−DMMP solution described in section III. The molecular model reproduces the experimental data reasonably. The depth of the minimum of DMMP mixing volume agrees with the experiment well and, in fact, is close to the literature value for DMSO.[29,30] The location of the minima is shifted to smaller DMMP concentrations, around 33% mol, which raises a concern that unphysical 1:2 DMMP−water complexes, which do not exist in reality, may be formed in the simulation (this issue is discussed below in section VI). Substantial deviations from the experiment are observed at higher DMMP molar fractions, above 0.5. The reason for this is unclear. We may speculate that this is related to the molecular structure of pure DMMP, which is somewhat different in experiments and simulations, but there are no experimental data available on the structure. The mixing enthalpy $\Delta\tilde{H}_{mix}$ in DMMP−water system follows the trend similar to that of $\Delta\tilde{V}_{mix}$: it has a minimum at 33 mol % DMMP, and its magnitude is approximately −2.9 kJ/mol, which is also close to $\Delta\tilde{H}_{mix}$ = −2.96 kJ/mol for DMSO. The results for two DMMP models applied in this work are similar, but the VN model[20] predicts less hydrophilic solvation and $\Delta\tilde{V}_{mix}$ shifted further away from the experimental data (see Supporting Information), which was expected since the SKCP model[22] assumes a stronger negative charge of the O(=P) oxygen atom compared to the VN model.

The solutions of both methylphosphonofluoridates behave similarly to DMMP solutions: the mixing volume and enthalpy are negative and have a minimum at compositions between 75 and 50 mol % water. Despite a similar charge of the O(=P) oxygen, the quantitative effect of mixing for sarin is substantially weaker than that of DMMP: the excess mixing volume for this system reaches only −0.55 cm^3/mol, and the enthalpy of mixing is above −2 kJ/mol. This may indicate that the size of the molecule and the overall volume of hydrophobic groups have a stronger effect on thermodynamic properties than the charge of the oxygen that serves as the main hydrogen bond acceptor. It is worth noting that *O*-methyl methylphosphonofluoridate, a smaller compound with a strong negative charge on the O(=P) oxygen also shows a very hydrophobic solvation with the excess mixing volume more negative than that for the DMMP—water mixture. Negative mixing volume was observed for soman and DIFP. These molecules are generally more hydrophobic, and the quantitative effect of solvation is generally smaller. The weakest effect is observed for DIFP, which has the least negative charge at the O(=P) oxygen.

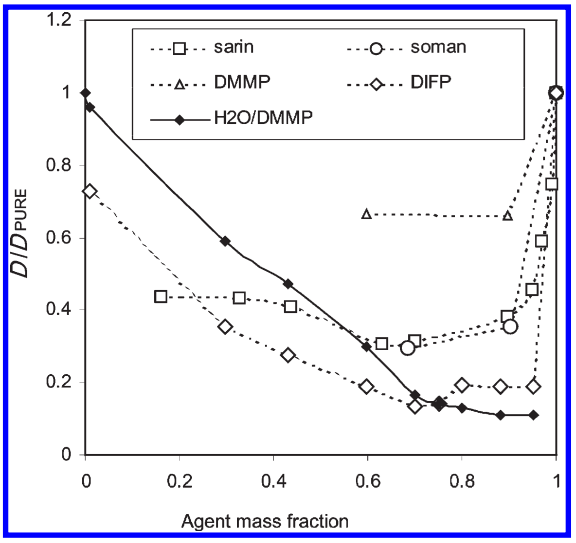

Figure 7. Self-diffusion coefficients of sarin, soman, DMMP, and DIFP in aqueous solutions related to the diffusion coefficients of pure chemicals. Filled diamonds show the water self-diffusion coefficient in the aqueous solutions of DMMP.

VI. SELF-DIFFUSION AND ITS DEPENDENCE ON MOLECULAR STRUCTURE

Self-diffusion coefficients were obtained from mean square displacement of the molecule center of mass using the Einstein relationship.[41] Figure 7 shows the diffusion coefficients reduced by the diffusion coefficient of pure components (listed in Table 3). For all four compounds, a characteristic dependence of the mobility on the composition is observed. Namely, the agent diffusion coefficient decreases sharply as water is added even in relatively small amounts (1−5 wt %). This is somewhat counterintuitive, since water as a solvent with smaller molecules and faster self-diffusion should generally facilitate diffusion of the heavier component. However, at low water concentrations, each water molecule forms two hydrogen bonds to the molecules of organophosphorous compounds.[42] These formations of one water molecule attached to two molecules of solute are well-defined, and their lifetime is much longer than the rotation correlation times of individual molecules. Since they are larger

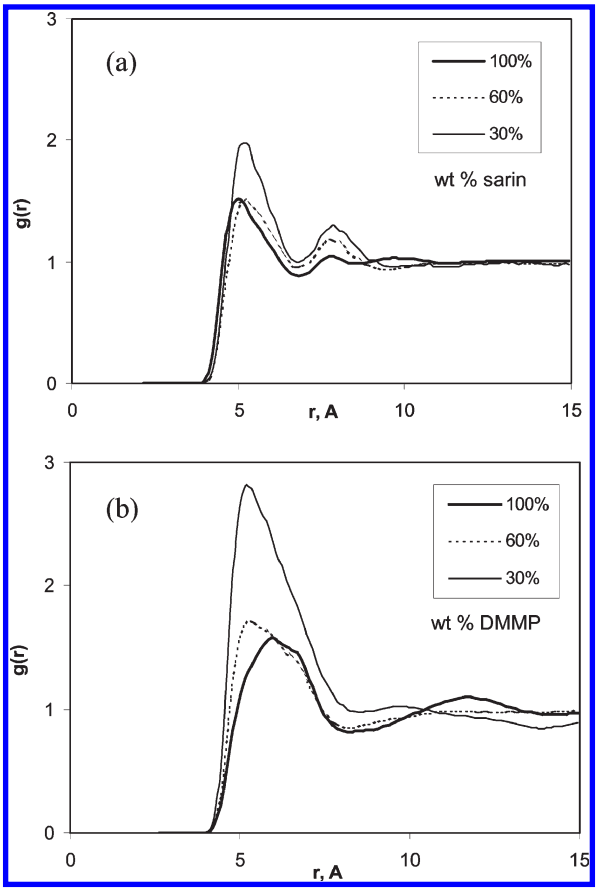

Figure 8. P—P radial distribution function in DMMP—water and sarin—water solutions at different mixture compositions.

than individual molecules, the diffusion in the entire system slows down. The average numbers of hydrogen bonds donated by a water molecule to other water and agent molecules showed no preference to O(═P) oxygens of the agents over the water oxygens. That is, O(═P) oxygens are about as attractive as hydrogen bond acceptors as water oxygens. The "ether" O(POC) oxygens as well as fluorines show much weaker hydrogen bonding, as expected. This 1:2 ratio results simply from an abundance of phosphororganic molecules in the solution and the geometry of water molecule, which has two available protons. As the number of available hydrogen bond donors increases with the water concentration, a wider network of hydrogen bonds is formed, which includes larger organophosphorous molecules and smaller water molecules. The extent of the network (basically, the number of accepted hydrogen bonds per phosphororganic molecule) and the average molecular size have opposite effects on the solute mobility. As a result, the diffusion coefficient of sarin and DMMP achieve minima at about 70% wt. Each water molecule nearly always donates two bonds, independent of the composition, and its self-diffusion coefficient monotonically decreases with the water concentration in the solution.

This complex behavior of thermodynamic and kinetic properties may also be related to the locally inhomogeneous structure of the solutions at higher water concentrations, which results from strongly polar P═O bond in otherwise rather hydrophobic molecules of sarin and DMMP. The inhomogeneous structure of their solutions is demonstrated by the RDFs for the phosphorus atoms of sarin and DMMP shown in Figure 8. The RDF peaks basically stay at the same positions as the water content increases, but the first peak becomes relatively higher, which clearly indicates a certain degree of DMMP and sarin aggregation in the solution. Such a behavior of RDFs might have indicated an unphysical liquid—liquid phase separation, inhibited by the periodic boundary conditions in our model system. However, such separation is extremely unlikely, for the strong negative mixing volume and high exposure of the O(═P) oxygens to water indicated by the number of hydrogen bonds. We may explain this observation by a strongly inhomogeneous, pseudo-micelle structure of the solutions: as the water fraction increases, the hydrophobic groups of the chemicals tend to cluster together, with the P═O bonds sticking outside into the surrounding water. This structure is visualized in the snapshots given in Figure 9. The inhomogeneity in DMMP solution is generally stronger than that in sarin solution (Figure 9a,b). DMMP and sarin essentially behave as "microlipids", though, due to their small size, these aggregates are not stable and cannot be characterized as genuine micelles or bilayers. The aggregation effect vanishes in the dilute solutions, where individual molecules of DMMP and sarin are surrounded by water, and the mobilities of DMMP and sarin increase. Similar quasi-aggregation is observed for water in soman and DIFP. Soman and DIFP are insoluble in water, but water shows a substantial solubility in either. Water tends to aggregate into small clusters as its concentration increases before the liquid—liquid phase separation occurs.

In order to check whether the scale of the inhomogeneity in the system is small enough so that the box size employed in simulatoions is sufficient, we performed NPT MD simulation of DMMP—water solution at 60 wt % DMMP in a larger box of 61 Å in average. The resulting density showed a very good agreement with $\rho = 1.113$ g/cm^3 obtained for the smaller system. The diffusion coefficients for both components turned out to be about 20% higher compared to the smaller system, which is natural as was shown in ref 43. Finally, the P—P and O_W—O_W RDFs for the two systems were essentially identical (these RDFs and final snapshots are shown in the Supporting Information). These results make us suggest that the box size of 35—40 Å is a reasonable minimum size required for such systems, and it is unlikely that simulations with a larger system size would make a dramatic affect on the results.

Although the inhomogeneous structure in the systems under consideration is well established, the available RDFs and other structural characteristics do not rule out possible existence of quasi-stable complexes formed by one DMMP (or sarin) and two or three water molecules. We attempted to characterize the complexation using the hydrogen bond lifetimes. If long-living 1:2 or 1:3 complexes exist in water—DMMP solutions, the hydrogen bonds donated by water to DMMP should be more stable compared to water—water hydrogen bonds. We used the same geometry criteria for the hydrogen bond: the hydrogen bond was considered as "established" when two oxygens were found at the distance less than 3.3 Å with OHO angle exceeding 120°. When the separation between these two oxygens exceeded 3.5 Å and/or the OHO angle became smaller than 100°, the hydrogen bond was counted as "broken". All "on-the-fly" hydrogen bonds that lived less than 2 ps (approximate rotational correlation time of a water molecule in the bulk at room temperature) were excluded from the averages. Despite a discretionary definition, the comparison of the average hydrogen bond lifetimes obtained this way should have revealed quasi-stable complexes. Attention was paid only to O(═P) oxygens of sarin and DMMP, since hydrogen

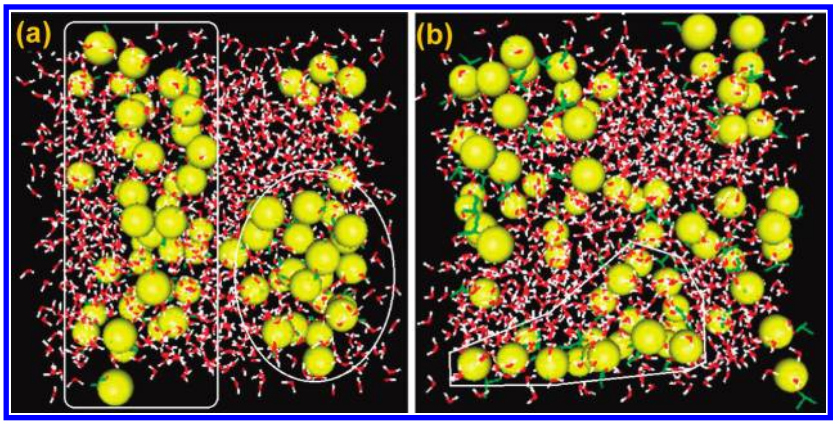

Figure 9. Snapshots for DMMP (a) and sarin (b) in water at 30 wt % (P atoms in large spheres). This figure illustrates the substantial degree of clustering in the system, as the component, whose concentration is lower (here presented in balls), "lumps together", which is also shown by RDFs (Figure 8). The strongly inhomogeneous structure is especially pronounce in DMMP solutions in water (Figure 9a). The "clusters" are shown by white markers.

bonding to the ether oxygens and fluorines was weak and the average hydrogen bond lifetime did not exceed 3 ps.

In diluted sarin−water solutions, the lifetimes of water−water and water−sarin hydrogen bonds are practically equal and close to 10 ps. This result indicates no complexes at low sarin concentrations. As sarin molar fraction increases, the hydrogen bond lifetime for bonds of both types increases monotonically and reaches a maximum at the same sarin concentration of 70 mol %, which generally corresponds to a minimum of sarin self-diffusion coefficient in this system. Sarin−water hydrogen bond average lifetime increases faster than that of water−water hydrogen bond at low sarin concentrations. At sarin molar fraction 0.091, their ratio is close to 1.6 (15.0−9.5 ps) and stays constant within the error margin for the remaining concentration range. The average lifetimes decline somewhat at high concentrations (from 30 and 45 ps at 70 mol % sarin to 24 and 40 ps at 92 mol % sarin, for water−water and water−sarin bonds, correspondingly). It is worth noting that the hydrogen bond lifetimes depend on the concentration similarly to sarin self-diffusion that shows a minimum at 70% sarin, and unlike water self-diffusion that declines monotonically with sarin molar fraction in the entire concentration range. Thus, the dynamic analysis of molecular geometry shows no sarin·$2H_2O$ or sarin·$3H_2O$ complex that would be drastically more stable than individual water−water hydrogen bonds. The results for DMMP−water system are similar. The only substantial difference is that the water−DMMP hydrogen bond lifetimes are longer than water−water ones throughout the entire concentration range, including dilute DMMP solutions.

VII. CONCLUSION

On the basis of the simulations with classical united-atom models, we conclude that DMMP and DIFP mimic the interactions of soman and sarin with water reasonably well. DMMP semiquantitatively represents a number of important properties of sarin, such as the excess mixing volume and enthalpy. On the basis of comparisons between DMMP and sarin, we conclude that alkylphosphonates of the same molecular size are generally more hydrophilic than G-agents. Correspondingly, as the size of attached alkyl groups increase, alkylphosphonates are better soluble in water than G-agents, which should be taken into account when the results obtained with simulants are projected onto G-agents. A stronger tendency of DMMP to inhomogeneity per se compared to that of sarin (Figures 8 and 9) should not be considered as a precursor to phase separation. On the other hand, judging from comparison between DIFP and soman properties, we may conclude that fluorophosphates are slightly less hydrophilic than corresponding G-agents, and their solubility is likely lower. Nevertheless, the simulants display the same complex dependence of the diffusion coefficient on the composition.

The inhomogeneous structure of the solution is particularly interesting with respect to behavior of G-agents and simulants in polyelectrolyte membranes. Both experiments[44,45] and simulations[21] independently showed that DMMP tends to concentrate in the fluoroether regions of nanosegregated Nafion membranes, forming a layer between the hydrophobic organic and hydrophilic aqueous subphases. This suggests that such behavior is intrinsic to agent sorption to polyelectrolytes and it results from a competition between agent−water interactions and agent−polymer interactions. This "quasi-segregated" morphology of a water−CWA mixture may be expected in any segregating polyelectrolyte or even in a nonsegregating polyelectrolyte that has a substantial amount of strongly hydrophobic groups, such as partially sulfonated polystyrene.

The forcefields employed in this study can be used for molecular modeling of competitive sorption of agents at ambient conditions with different humidities with the fluid−solid interaction potentials fitted to the adsorption isotherms of individual components.

■ ASSOCIATED CONTENT

Supporting Information. Figures showing bond stretching energies and angular terms for DIFP and comparison of VN and SKCP models for DMMP. This material is available free of charge via the Internet at http://pubs.acs.org.

■ AUTHOR INFORMATION

Corresponding Author
*E-mail: aneimark@rutgers.edu.

■ ACKNOWLEDGMENT

The authors are thankful to C. Karwacki, B. Schindler (Edgewood Chemical & Biological Center, Aberdeen, MD), and N. Schneider

(U.S. Army Soldier RD&E Center, Natick, MA) for fruitful discussions. Several simulations of sarin−water systems were performed by Christopher Papamitrou. This work was supported in parts by DTRA (Grant HDTRA1-08-1-0042) and ARO (Grant W911NF-09-1-0242).

REFERENCES

(1) Frishman, G.; Amirav, A. *Field Anal. Chem. Technol.* **2000**, *4*, 170.
(2) Suzin, Y.; Nir, I.; Kaplan, D. *Carbon* **2000**, *38*, 1129.
(3) Vo-Dinh, T.; Stokes, D. L. *Field Anal. Chem. Technol.* **1999**, *3*, 346.
(4) Arbuzov, B. A.; Shavsha, T. G. *Izv. Akad. Nauk SSSR, Ser. Khim.* **1952**, 875.
(5) Arbuzov, B. A.; Vinogradova, V. S. *Izv. Akad. Nauk SSSR, Ser. Khim.* **1952**, 865.
(6) Kosolapoff, G. M. *J. Chem. Soc.* **1954**, 3222.
(7) Kosolapoff, G. M. *J. Am. Chem. Soc.* **1954**, *76*, 615.
(8) Ewig, C. S.; van Wazer, J. R. *J. Mol. Struct.: THEOCHEM* **1985**, *122*, 179.
(9) Suenram, R. D.; Lovas, F. J.; Plusquellic, D. F.; Lesarri, A.; Kawashima, Y.; Jensen, J. O.; Samuels, A. C. *J. Mol. Spectrosc.* **2002**, *211*, 110.
(10) Walker, A. R. H.; Suenram, R. D.; Samuels, A.; Jensen, J.; Ellzy, M. W.; Lochner, J. M.; Zeroka, D. *J. Mol. Spectrosc.* **2001**, *207*, 77.
(11) Ault, B. S.; David, A. B.; Tevault, D.; Hurley, M. *J. Phys. Chem. A* **2004**, *108*, 10094.
(12) Bermudez, V. M. *J. Phys. Chem. C* **2007**, *111*, 9314.
(13) Bermudez, V. M. *J. Phys. Chem. C* **2007**, *111*, 3719.
(14) Bermudez, V. M. *J. Phys. Chem. C* **2010**, *114*, 3063.
(15) Barvik, I.; Stepanek, J.; Bok, J. *Czech. J. Phys.* **1998**, *48*, 409.
(16) Barvik, I.; Stepanek, J.; Bok, J. *J. Biomol. Struct. Dyn.* **2002**, *19*, 863.
(17) Bencsura, A.; Enyedy, I.; Kovach, I. M. *Biochemistry* **1995**, *34*, 8989.
(18) Bencsura, A.; Enyedy, I. Y.; Kovach, I. M. *J. Am. Chem. Soc.* **1996**, *118*, 8531.
(19) Soliva, R.; Monaco, V.; Gomez-Pinto, I.; Meeuwenoord, N. J.; Van der Marel, G. A.; Van Boom, J. H.; Gonzalez, C.; Orozco, M. *Nucleic Acids Res.* **2001**, *29*, 2973.
(20) Vishnyakov, A.; Neimark, A. V. *J. Phys. Chem. A* **2004**, *108*, 1435.
(21) Rivin, D.; Meermeier, G.; Schneider, N.; Vishnyakov, A.; Neimark, A. V. *J. Phys. Chem. B* **2004**, *108*, 8900.
(22) Sokkalingam, N.; Kamath, G.; Coscione, M.; Potoff, J. J. *J. Phys. Chem. B* **2009**, *113*, 10292.
(23) Lu, X. Y.; Nguyen, V.; Zeng, X. H.; Elliott, B. J.; Gin, D. L. *J. Membr. Sci.* **2008**, *318*, 397.
(24) Dunning, T. H. *J. Chem. Phys.* **1989**, *90*, 1007.
(25) Becke, A. D. *J. Chem. Phys.* **1993**, *98*, 5648.
(26) Stephens, P. J.; Devlin, F. J.; Chabalowski, C. F.; Frisch, M. J. *J. Phys. Chem.* **1994**, *98*, 11623.
(27) Pulay, P.; Baker, J.; Wolinski, K. *PQS, version* 3.3: Parallel Quantum Solutions: Fayetteville, AR, 1997.
(28) Hess, B.; Kutzner, C.; van der Spoel, D.; Lindahl, E. *J. Chem. Theory Comput.* **2008**, *4*, 435.
(29) Cowie, J. M. G.; Toporowski, P. M. *Can. J. Chem.* **1961**, *39*, 2240.
(30) Kenttamaa, J.; Lindberg, J. J. *Suom. Kemistil. B* **1960**, *33*, 98.
(31) Glättli, A.; Oostenbrink, C.; Daura, X.; Geerke, D. P.; YuI, H.; vanGunsteren, W. F. *Braz. J. Phys* **2004**, *34*, 116.
(32) Vishnyakov, A.; Lyubartsev, A. P.; Laaksonen, A. *J. Phys. Chem. A* **2001**, *105*, 1702.
(33) Lyubartsev, A. P.; Laaksonen, A. *Comput. Phys. Commun.* **2000**, *128*, 565.
(34) Berendsen, H. J. C.; Grigera, J. R.; Straatsma, T. P. *J. Phys. Chem.* **1987**, *91*, 6269.
(35) Verlet, L. *Phys. Rev.* **1967**, *159*, 98.
(36) Tuckerman, M.; Berne, B. J.; Martyna, G. J. *J. Chem. Phys.* **1992**, *97*, 1990.
(37) Hoover, W. G. *Phys. Rev. A* **1985**, *31*, 1695.
(38) Nose, S. *Mol. Phys.* **1984**, *52*, 255.
(39) Bartelt-Hunt, S. L.; Knappe, D. R. U.; Barlaz, M. A. *Crit. Rev. Environ. Sci. Technol.* **2008**, *38*, 112.
(40) Preston, J. M.; Starrock, V. *Partial vapour pressures and activity coefficients of GB and GD in aqueous solution*, 1983.
(41) Landau, L. D.; Lifshitz, E. M. *Fluid Mechanics*, 2nd ed.; Pergamon Press: New York, 1987; Vol. 6, Course of Theoretical Physics.
(42) Lyubartsev, A. P.; Laaksonen, A. *J. Biomol. Struct. Dyn.* **1998**, *16*, 579.
(43) Yeh, I.-C.; Hummer, G. *J. Phys. Chem. B* **2004**, *108*, 15873.
(44) Giotto, M. V.; Zhang, J. H.; Inglefield, P. T.; Wen, W. Y.; Jones, A. A. *Macromolecules* **2003**, *36*, 4397.
(45) Meresi, G.; Wang, Y.; Bandis, A.; Inglefield, P. T.; Jones, A. A.; Wen, W. Y. *Polymer* **2001**, *42*, 6153.
(46) Stubbs, J. M.; Potoff, J. J.; Siepmann, J. I. *J. Phys. Chem. B* **2004**, *108*, 17596.
(47) Langford, R. E. *Introduction to Weapons of Mass Destruction-Radiological, Chemical and Biological*; John Wiley & Sons: Hoboken, NJ, 2004.
(48) Silver, S. D. *J. Ind. Hyg. Toxicol.* **1948**, *30*, 307.
(49) *The Merck Index: An Encyclopedia of Chemicals, Drugs, and BiologicalsMerck Index*, 11th ed.; Budavari, S., Ed.; Merck & Co.: Rahway, NJ, 1989; p 814.